Radar Tracking Performance When Sensing and Processing Compressive Measurements

Ioannis Kyriakides
Department of Engineering
University of Nicosia
Nicosia, Cyprus
kyriakides.i@unic.ac.cy

Abstract − *Radar tracking performance is improved when using waveforms at high delay-Doppler resolution with concentrated ambiguity functions. High resolution measurement acquisition and processing, however, requires high rate sampling and intensive processing. Alternatively, compressive sensing and processing can be used to significantly reduce data rates with no loss in resolution. The drawback is, however, that using compressive measurements increases ambiguity function sidelobes and thus tracking error.*

In this paper, compressive sensing and processing is applied to single target tracking. The effect of compressive sensing and processing on the ambiguity function sidelobes is examined. Moreover, estimation using compressively sampled and processed Björck CAZAC sequences is shown to be improved over estimation using linear frequency modulated waveforms sampled at the Nyquist rate. This shows that low-rate acquisition and processing maintains reliable tracking performance at high resolution, while simplifying the receiver and reducing computational expense.

Keywords: Tracking, filtering, estimation, compressive sensing.

1 Introduction

Radar tracking performance depends on the shape of the ambiguity function (AF) [1] of the waveform used and on the delay-Doppler resolution of the radar measurements. Using waveforms with AFs that are well concentrated in the origin and have small sidelobes increases certainty in delay-Doppler localization [1]. Moreover, the ability to form hypotheses of target range and range rate on a fine grid of delay-Doppler bins results to higher tracking accuracy. There is, however, a tradeoff between the resolution of an AF and its sidelobe levels. This is due to limitations in the radar receiver and processing unit.

Specifically, high resolution tracking requires both high data rate measurement acquisition and processing of long discrete-time sequences. This places heavy demands on the analog to digital converter at both the receiver [2] and the processor, especially when using a particle filter based method [3]. To reduce the sampling and processing rate requirements *compressive sensing* [4, 5, 6, 2, 7, 8] and *compressive processing* [9, 10] have been proposed.

Compressive sensing enables the analog to information conversion of signals that are sparse in some basis or dictionary, sampling them well below the Nyquist rate. Reconstruction of the signal [11, 12, 13] can then reveal its sparse components. In a radar application, for example, when the received signal is a delayed and Doppler shifted version of the transmitted waveform, it is then sparse in a dictionary made up of delayed and Doppler shifted versions of the waveform. This dictionary is, however, sparsifying only if it is made up of delayed and Doppler shifted waveforms that are nearly orthogonal. This is true for waveforms with AFs with very low sidelobes (representing low correlations between dictionary elements) such as the Björck CAZAC [14, 15, 16]. In order to build the sparsifying dictionary a finite set of possible delay and Doppler shifts can be derived from the target model or operation requirements of a specific radar tracking scenario at hand. Compressive sensing of the received signal will then preserve information on the target range and range rate contained in the return signal while simplifying receiver design.

If compressive sensing of high resolution measurements is followed by *compressive processing* then the computationally intensive reconstruction processes and the processing of long data sequences are avoided. Instead, processing is performed using the compressive samples which are much less in number than the Nyquist rate samples. Compressive processing, however, results to an increase in estimation error as compared to processing the recovered signal or the signal sampled at Nyquist [9, 10]. In a delay-Doppler estimation problem, the estimation error is due to an increase in the sidelobes of the AF associated with the trans-

mitted waveform. This AF structure deterioration will in turn increase tracking error. A natural first step to improving tracking performance with compressed measurements is to use waveforms with sidelobes lower than the ones of the traditionally used linear frequency modulated (LFM) waveforms at delay-Doppler locations of interest. One example of such a waveform is the Björck CAZAC. The use of Björck CAZACs as radar waveforms has recently been proposed in [14] where improvement in tracking performance over the use of LFMs was reported.

In this paper, the feasibility of using compressive sensing and processing in target state estimation with a particle filter is investigated. To this end, the AFs of large length LFM and CAZAC sequences are compared to the AFs of LFM and CAZAC waveforms that are compressively sensed. Moreover, the tracking error when using compressed sensing and a Björck CAZAC sequence is compared to the error when acquiring radar returns at the Nyquist rate. Numerical results show that the tracking performance when using compressively sensed and processed CAZAC sequences is deteriorated compared to using ideal Nyquist sampled CAZACs. However, tracking with compressed CAZACs still outperforms tracking using Nyquist sampled LFMs. This provides sufficient evidence that using compressive measurements without reconstruction provides reliable tracking while enabling high resolution/low rate measurement acquisition and processing. Moreover, the results create interest for further research in the concept of AF design considering not just the waveform, but also the method of sensing radar measurements.

This paper is organized as follows. In Section 2 the construction of a dictionary made up of delayed and Doppler shifted Björck CAZAC sequences is demonstrated and the compressive measurement acquisition matrix is presented. In Section 3 the AF when using compressive measurements is presented and the LFM and CAZAC waveform AFs, when sampling and processing either at Nyquist or compressively, are compared. In Section 4 the motion and measurement models are provided and the statistical parameters of the matched filter statistic when measurements are acquired compressively are derived. In Section 5 the tracking scenario and the numerical results on the tracking performance and the ability to reconstruct the compressively sampled CAZAC waveform are presented. Finally, in Section 6 general conclusions are drawn and future work is outlined.

2 Delay-Doppler sparsity and incoherence with sensing matrix

In this section the sparsity of the Björck CAZAC radar waveform with reference to a dictionary of delayed and Doppler shifted versions of the waveforms is explored. Moreover, the sensing matrix used for compressively acquiring the radar waveform, that needs to be incoherent with the dictionary, is demonstrated. Based on the conditions of sparsity and incoherence [5] the delay and Doppler shift information in the return waveform is preserved. This is also demonstrated by the waveform reconstruction using the SPGL1 algorithm [13] in Section 5.

2.1 Sparsifying dictionary construction

A radar sensor transmits a waveform $s(m), m = 0, \ldots, M-1$, where M is the total number of samples of the waveform. It then receives the return waveform after it is reflected from a target at a certain range r and range-rate $\dot{r}$. As explained in more detail in Section 4.2, the received waveform is modeled as a delayed and Doppler shifted version of the transmitted waveform by a discrete delay τ and Doppler ν, that are proportional to the range and range-rate of the target, as

$$s_{\tau,\nu}(m) = s(m-\tau)e^{j2\pi m\nu/M_d}, m = 0, \ldots, M_d - 1$$

where the random scaling and noise terms (see Section 4.2) have been omitted for simplicity in the present discussion. Moreover, $M_d > M$ is chosen to be large enough to accommodate the maximum delay of a signal reflected from a target.

The possible delay and Doppler shifts that the transmitted waveform can undergo after being reflected off a target form a *finite* set. This set is limited by the minimum and maximum range and range-rate values of operation of the radar system and the target motion. In order to perform acquisition at a sub-Nyquist rate while preserving information a necessary condition is that the received waveform is sparse in some basis or dictionary [17].

In this work the sparsifying dictionary is composed of the finite set of delayed and Doppler-shifted waveforms described above. The dictionary can be expressed in the form of a matrix $\mathbf{S}$ with columns the M_d length vectors $\mathbf{s}_{\tau,\nu}$ with indices $s_{\tau,\nu}(m), m = 1, \ldots, M_d - 1$. Here, $\mathbf{s}_{\tau,\nu}$ has been zero padded by appending zeros in order to increase the length of $s(m), m = 1, \ldots, M-1$ from M to M_d. Assuming that the radar receiver starts acquiring the return waveform when the minimum expected delayed version of the signal may arrive τ_{min}, which is set to zero with no loss of generality, the number of zeros to be appended equals the maximum possible delay index τ_{max}. By varying τ in the expression above from 0 to τ_{max} the dictionary is provided with all the possible delays. Moreover, for every delay, the dictionary is provided with a range of discrete Doppler-shifts $\nu = \nu_{min}, \ldots, \nu_{max}$. Therefore, $\mathbf{S}$ becomes a matrix of $M_d = M + \tau_{max}$ rows. The number of columns is $S_{col} = (\tau_{max} + 1) \times (\nu_{max} - \nu_{min} + 1)$ which is equal to the product of the number of delay and Doppler shifts possible.

Based on the above, the sparse column vector $\mathbf{s}_{sp}$ with indices $s_{sp}(m), m = 0, \ldots, S_{col} - 1$ obtained when projecting the received signal $\mathbf{s}$ onto the dictionary is given in matrix form as $\mathbf{s}_{sp} = \mathbf{S}^*\mathbf{s}^T$ where $(*)$ and (T) denote the conjugate transpose and the transpose operation respectively. The number of non-zero sparse coefficients in $\mathbf{s}_{sp}$ is denoted as $\mathcal{S}$ out of $S_{col} = (\tau_{max} + 1) \times (\nu_{max} - \nu_{min} + 1)$ total coefficients. The above projection is equivalent to correlating the received signal to the dictionary columns. Therefore, the values of $\mathbf{s}_{sp}$ are in fact the values of the AF of $s(m)$ at the respective delay and Doppler locations. The AF is presented formally in Section 3.

In this paper tracking is performed using the LFM and Björck CAZAC (see [14, 15, 16] for more detail on the waveforms). For the Björck CAZAC, the correlation between the columns of the dictionary is very small, since the AF sidelobes are very small (see Figure 1). Therefore, a dictionary based on the Björck CAZAC is nearly orthogonal and is a good candidate for a sparsifying dictionary that can be used to reconstruct the sparse coefficients. An LFM dictionary, however, exhibits higher correlations (see the LFM AF in Figure 4). Therefore, the LFM dictionary is not recommended for use as a sparsifying dictionary for reconstructing LFM radar waveforms.

2.2 Measurement acquisition matrix

The radar sensing matrix $\mathbf{\Phi}$ is, in this work, a matrix with entries $\Phi(c, m)$ with rows and columns with indices $c = 0, \ldots, C - 1$ and $m = 0, \ldots, M_d - 1$ respectively. In order to create the entries of $\mathbf{\Phi}$ independent samples from a Gaussian distribution with mean zero and variance 1 are taken. This is followed by orthogonal-triangular decomposition [13] to create an orthogonal and normalized $\mathbf{\Phi}$. Therefore, $\mathbf{\Phi}$ is now made up of zero mean $\frac{1}{M_d}$ variance Gaussian entries. Moreover, the rows of $\mathbf{\Phi}$ are orthogonal, that is $\sum_{m=0}^{M_d-1} \Phi(c, m)\Phi^*(c', m)$ is equal to 1 for $c = c'$ and 0 otherwise. Alternatively, a quasi-Toeplitz matrix with Gaussian distributed entries can be used for a more realistic receiver design [7]. A matrix with Gaussian entries is shown in [4, 6, 18] to be incoherent with any fixed basis [7]. Therefore, the compressive sampling process will preserve the sparsity in the received radar signal that belongs to a dictionary of CAZAC waveforms mentioned above.

In order to show that the information in the received signal is preserved with the randomly generated matrix, the noiseless version of the received signal is reconstructed in Section 5 for a different number of acquired compressive measurements. The minimum number of compressive measurements required for reconstruction agrees with the relationship $C \geq \alpha \mathcal{S} \log(M_d/\mathcal{S})$, where α is a constant, provided in [5]. This relationship holds for the choice of the randomly generated acquisition matrix described above. The ability to reconstruct the return waveform additionally demonstrates that the CAZAC dictionary is suitable as a sparsifying dictionary.

The goal in this work is, however, to estimate the target state using the compressed measurements with no reconstruction. Therefore, the reconstruction results provided are only used to demonstrate that the delay-Doppler information when using the Björck CAZAC is safely embedded in the compressive measurements.

3 Compressive sensing and ambiguity functions

In this section the AF sidelobe behavior of the LFM and Björck CAZAC for the case where the two waveforms are sampled at the Nyquist rate and for the case when they are compressively sampled is examined. In [14, 15, 16] more detail on the waveforms is provided. When a waveform $s(m), m = 0, \ldots, M - 1$ is sampled at Nyquist, where M is the total number of Nyquist samples, the associated AF, is given by [19]:

$$\mathcal{A}(\tau, \nu) = \frac{1}{\xi} \sum_{m=0}^{M_d-1} s_{\tau,\nu}(m) s^*(m) \tag{1}$$

where

$s_{\tau,\nu}(m) = s(m - \tau) e^{j2\pi m\nu/M_d}, m = 0, \ldots, M_d - 1$ is a delayed by τ and Doppler shifted by ν version of $s(m), m = 0, \ldots, M - 1$ and

$$\xi = \sum_{m=0}^{M-1} s(m) s^*(m) \tag{2}$$

is the energy of the transmitted signal. Next, the compressive sampling of the waveform and the resulting AF is described.

The compressive sampling procedure is equivalent to multiplying a vector $s_{\tau,\nu}(m), m = 0, \ldots, M_d - 1$ (that is sparse in a dictionary of interest) with an $C \times M_d$, $C < M_d$ acquisition matrix $\mathbf{\Phi}$, described in Section 2.2, that is incoherent with the dictionary [4, 6]. The compressively sensed vector resulting from this projection is given by:

$$s_{cs,\tau,\nu}(c) = \sum_{m=0}^{M_d-1} \Phi(c, m) s_{\tau,\nu}(m), c = 0, \ldots, C - 1 \tag{3}$$

where C represents the number of compressive samples acquired. In the above, a number of compressive measurements C is taken that is much less than the number of Nyquist measurements M_d. The compressed waveform energy with respect to the transmitted waveform energy is, using the restricted isometry property [10, 20, 5],

$$\xi_{cs} = \sum_{c=0}^{C-1} s_{cs}(c) s_{cs}^*(c) = \beta \frac{C}{M_d} \xi \tag{4}$$

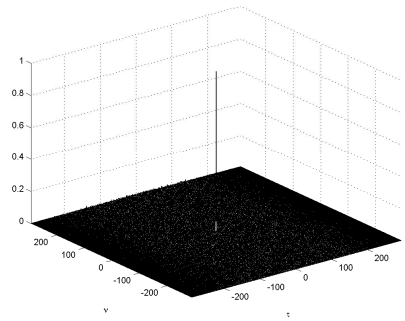

Figure 1: AF of a Björck CAZAC sequence with $M = 293$.

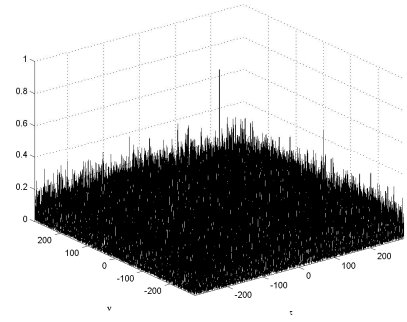

Figure 2: AF of a compressively sensed $M = 293$ length Björck CAZAC sequence with $C = 20$ samples.

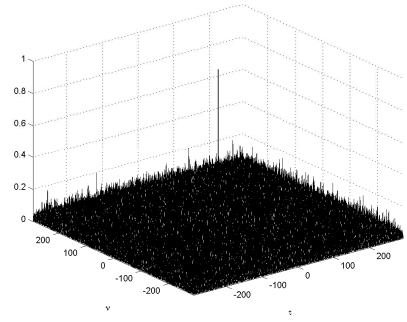

Figure 3: AF of a compressively sensed $M = 293$ length Björck CAZAC sequence with $C = 50$ samples.

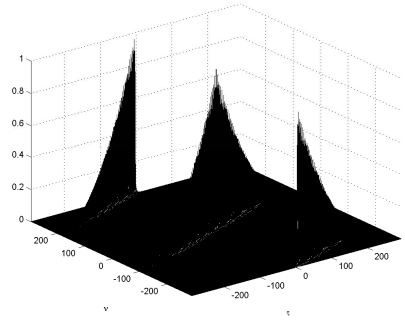

Figure 4: AF of a LFM sequence with $M = 293$.

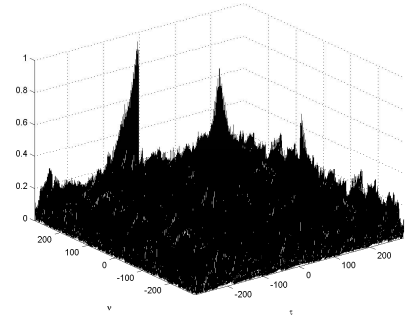

Figure 5: AF of a compressively sensed $M = 293$ length LFM sequence with $C = 20$ samples.

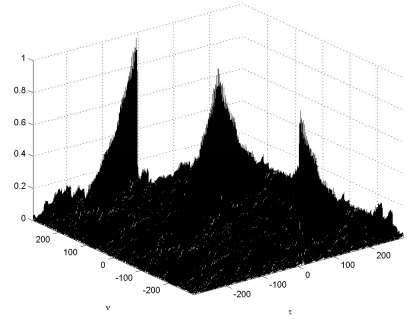

Figure 6: AF of a compressively sensed $M = 293$ length LFM sequence with $C = 50$ samples.

with $1 - \delta \leq \beta \leq 1 - \delta$ where $\delta \in (0, 1)$ is the restricted isometry constant. In order to obtain the AF the compressed waveforms are correlated as

$$\mathcal{A}_{cs}(\tau, \nu, \bar{\tau}, \bar{\nu}) = \frac{M_d}{\beta C \xi} \sum_{c=0}^{C-1} s_{cs,\tau,\nu}(c) s^*_{cs,\bar{\tau},\bar{\nu}}(c) \qquad (5)$$

where $\frac{M_d}{\beta C \xi}$ is the energy normalization factor. As seen above, the compressed AF is 4-dimensional as opposed to the Nyquist AF that varies with respect to the difference between the delays and Doppler shifts of the waveforms. For the purposes of studying the increase in the AF sidelobes due to compressive processing $\bar{\tau}$ and $\bar{\nu}$ are set to zero in this work for simplicity. Further work will study the effect of Φ on the compressed AF and the symmetries that it exhibits. The goal is to develop adaptive schemes for shaping the AF to improve tracking performance.

The AFs of the LFM and a Björck CAZAC, both of length $M = 293$, are shown in Figures 1 and 4 respectively. Comparing the two figures it is immediately obvious that using a Björck CAZAC versus an LFM reduces ambiguity in delay and Doppler in the area of interest of a particle filter based tracker, which is near the origin of the AF [14]. The AFs of the Björck CAZAC sensed with different numbers of compressive measurements $C = 20, 50$ are shown in Figures 2 and 3 respectively. The AFs of compressively sensed LFM's are shown in Figures 5 and 6. The figures mentioned above demonstrate the degradation in the waveform's AF shape as the number of samples acquired are reduced.

4 Tracking scenario

4.1 Motion model

As in [14] this paper considers a single target moving in a two-dimensional plane. The dynamics of the target are modeled using a nearly constant velocity motion model in Cartesian coordinates. Specifically, the state vector for the target at the time step k, $k = 1, ..., K$, of the scenario is given by: $\mathbf{x}_k = [x_k\ \dot{x}_k\ y_k\ \dot{y}_k]^T$, where x_k, y_k are the positions in the x and y coordinates, and $\dot{x}_k$, $\dot{y}_k$ are the corresponding velocities. The motion is formulated as:

$$\mathbf{x}_k = \mathbf{F}\mathbf{x}_{k-1} + \mathbf{Q}\mathbf{v}_{k-1}, \qquad (6)$$

where $\mathbf{F} = [1\ \delta t\ 0\ 0; 0\ 1\ 0\ 0; 0\ 0\ 1\ \delta t; 0\ 0\ 0\ 1]$ and δt is the time difference between state transitions. The matrix $\mathbf{Q}$ is the process noise covariance matrix, and $\mathbf{v}_k$ denotes a zero-mean, unit variance Gaussian process that models errors in velocity, possibly due to unknown acceleration; in this work, $\mathbf{Q}$ is restricted to be diagonal. The model in (6) can be used to determine the kinematic prior distribution $p(\mathbf{x}_k|\mathbf{x}_{k-1})$.

4.2 Measurement model

The measurement model used in this paper follows the one in [14]. Here it is outlined briefly, focusing more on deriving the statistical parameters of the compressively sensed waveform.

A radar system collects information regarding the range and range rate of a target relative to the radar sensors by transmitting signal pulses and processing the return. The return signal bears information on the range of a target relative to a sensor $u = 1, \ldots, U$ of the radar system in the form of a time delay and on the range rate in the form of a Doppler shift. Every time step k a radar waveform $s(m), m = 0, \ldots, M-1$, where M is the total number of samples of the waveform, is transmitted from U sensors. In this work, the assumption is that the same waveform is simultaneously transmitted from each sensor. Moreover, the sensors are appropriately positioned to provide different view-points of the target so that the target state in the Cartesian coordinates can be inferred from the range and range-rate readings given by each sensor [14]. The return signals that are reflected from the target with a delay $\tau_{u,k}$ and Doppler $\nu_{u,k}$ arriving at the sensors are:

$$d_{u,k}(m) = A_k s(m - \tau_{u,k}) e^{j2\pi m \nu_{u,k}/M_d} + v_{u,k}(m) \quad (7)$$

for $m = 0, \ldots, M_d - 1$, where A_k is a sum of random complex returns from many different target scatterers, according to the Swerling I model [21, 22], and with $M_d > M$ chosen to be large enough to accommodate the maximum delay of a signal reflected from a target. Therefore, A_k is assumed to be zero-mean, complex Gaussian with known variance $2\sigma_A^2$ and $v_{u,k}(m)$ to be a zero-mean complex Gaussian noise with variance $2N_0$.

The return signal is passed through matched filters with different delay and Doppler shifts for each sensor u, derived from the belief in target state as in [14]. For example, one of the delay and Doppler shifts at sensor u at time step k is denoted as $\bar{\tau}_{u,k}$ and $\bar{\nu}_{u,k}$ respectively, giving rise to the matched signal $s_{\bar{\tau},\bar{\nu},u,k}(m) = s(m - \bar{\tau}_{u,k}) e^{j2\pi m \bar{\nu}_{u,k}/M_d}$. The output matched filter statistic is given by:

$$\mathbf{y}_{\bar{\tau},\bar{\nu},u,k} = |\tilde{\mathbf{y}}_{\bar{\tau},\bar{\nu},u,k}|^2$$

where

$$\tilde{\mathbf{y}}_{\bar{\tau},\bar{\nu},u,k} = \sum_{m=0}^{M_d-1} d_{u,k}(m) s^*_{\bar{\tau},\bar{\nu},u,k}(m).$$

Substituting for $d_{u,k}(m)$ in (7), using (1), and letting $\Delta\tau_{u,k} = \tau_{u,k} - \bar{\tau}_{u,k}, \Delta\nu_{u,k} = \nu_{u,k} - \bar{\nu}_{u,k}$ we have that

$$\tilde{\mathbf{y}}_{\bar{\tau},\bar{\nu},u,k} = A_k \xi \mathcal{A}(\Delta\tau_{u,k}, \Delta\nu_{u,k}) + \sum_{m=0}^{M_d-1} v_{u,k}(m) s^*_{\bar{\tau},\bar{\nu},u,k}(m). \quad (8)$$

$\tilde{\mathbf{y}}_{\bar{\tau},\bar{\nu},u,k}$ is zero mean complex Gaussian with variance [19]:

$$\sigma_1^2 = 2\sigma_A^2 \xi^2 |\mathcal{A}(\Delta\tau_{u,k}, \Delta\nu_{u,k})|^2 + 2N_0\xi. \quad (9)$$

Below the proof of (9) is outlined. The proof for the continuous time case is given in [19]. The variance of $\tilde{\mathbf{y}}_{\bar{\tau},\bar{\nu},u,k}$ when the target is present is given by

$$\sigma_1^2 = E[\tilde{\mathbf{y}}_{\bar{\tau},\bar{\nu},u,k} \tilde{\mathbf{y}}^*_{\bar{\tau},\bar{\nu},u,k}]$$

which using (8) and the independence of A_k and $v_{u,k}(m)$ becomes

$$\sigma_1^2 = E[(A_k \xi \mathcal{A}(\Delta\tau_{u,k}, \Delta\nu_{u,k}) A_k^* \xi \mathcal{A}^*(\Delta\tau_{u,k}, \Delta\nu_{u,k}))] + E[(\sum_{m=0}^{M_d-1} v_{u,k}(m) s^*_{\bar{\tau},\bar{\nu},u,k}(m))(\sum_{m=0}^{M_d-1} v^*_{u,k}(m) s_{\bar{\tau},\bar{\nu},u,k}(m))]$$

which further using the independence of $v_{u,k}(m)$ and $v_{u,k}(m')$, $m \neq m'$

$$\sigma_1^2 = E[A_k A_k^*] \xi^2 \mathcal{A}(\Delta\tau_{u,k}, \Delta\nu_{u,k}) \mathcal{A}^*(\Delta\tau_{u,k}, \Delta\nu_{u,k}) + \sum_{m=0}^{M_d-1} E[v_{u,k}(m) v^*_{u,k}(m)] s^*_{\bar{\tau},\bar{\nu},u,k}(m) s_{\bar{\tau},\bar{\nu},u,k}(m)$$

where using $2\sigma_A^2 = E[(A_k A_k^*)]$, $2N_0 = E[v_{u,k}(m) v^*_{u,k}(m)]$, and (2) then relation (9) follows:

$$\sigma_1^2 = 2\sigma_A^2 \xi^2 |\mathcal{A}(\Delta\tau_{u,k}, \Delta\nu_{u,k})|^2 + 2N_0\xi.$$

Similarly, if no target is present $\sigma_0^2 = 2N_0\xi$. Based on the above, the matched filter statistic $\mathbf{y}_{\bar{\tau},\bar{\nu},u,k} = |\tilde{\mathbf{y}}_{\bar{\tau},\bar{\nu},u,k}|^2$ is exponentially distributed. Therefore,

$$p(\mathbf{y}_{\bar{\tau},\bar{\nu},u,k} | \mathbf{x}_k) = \begin{cases} \frac{1}{2\sigma_1^2} e^{-\frac{\mathbf{y}_{\bar{\tau},\bar{\nu},u,k}}{2\sigma_1^2}}, & \text{if target present} \\ \frac{1}{2\sigma_0^2} e^{-\frac{\mathbf{y}_{\bar{\tau},\bar{\nu},u,k}}{2\sigma_0^2}}, & \text{if target not present.} \end{cases}$$

If the matched filter output is thresholded, we have:

$$\bar{\mathbf{y}}_{\bar{\tau},\bar{\nu},u,k} = \begin{cases} 1, & \text{if } \mathbf{y}_{\bar{\tau},\bar{\nu},u,k} \geq \mathcal{T} \\ 0, & \text{if } \mathbf{y}_{\bar{\tau},\bar{\nu},u,k} < \mathcal{T} \end{cases}$$

obtaining a detection (1) or no detection (0). The threshold is given by $\mathcal{T} = -2\sigma_0^2 \ln(P_f)$, where ln is the natural logarithm, and P_f is the probability of false alarm. The probability of detection is given by $P_d = P_f^{1/(1+\text{SNR } A(\Delta\tau_{u,k}, \Delta\nu_{u,k}))}$. The signal-to-noise ratio (SNR) at the output of the matched filter is defined as $\text{SNR} = \frac{\sigma_A^2 \xi}{N_0}$ [19].

Next, a similar analysis is performed for the case of sensing the received waveform compressively. The compressively sensed measurement is

$$d_{cs,u,k}(c) = \sum_{m=0}^{M_d-1} \Phi(c, m) d_{u,k}(m), c = 0, \ldots, C-1$$

with $M_d > M$ again chosen to accommodate a maximum delay of a signal reflected from a target. Using (7) and (3) we have that

$$d_{cs,u,k}(c) = As_{cs,\tau,\nu,u,k}(c) + \sum_{m=0}^{M_d-1} \Phi(c,m)v_{u,k}(m), \tag{10}$$

$$c = 0, \ldots, C-1.$$

The matched filter statistic now becomes

$$\mathbf{y}_{cs,\bar{\tau},\bar{\nu},u,k} = |\tilde{\mathbf{y}}_{cs,\bar{\tau},\bar{\nu},u,k}|^2$$

where $\tilde{\mathbf{y}}_{cs,\bar{\tau},\bar{\nu},u,k} = \sum_{c=0}^{C-1} d_{cs,u,k}(c)s^*_{cs,\bar{\tau},\bar{\nu},u,k}(c)$ which using (10), (5), and (4) becomes

$$\tilde{\mathbf{y}}_{cs,\bar{\tau},\bar{\nu},u,k} = A\frac{\beta C\xi}{M_d}\mathcal{A}_{cs}(\tau_{u,k},\nu_{u,k},\bar{\tau}_{u,k},\bar{\nu}_{u,k})$$

$$+\sum_{c=0}^{C-1}\sum_{m=0}^{M_d-1}\Phi(c,m)v_{u,k}(m)s^*_{cs,\bar{\tau},\bar{\nu},u,k}(c)$$

$\tilde{\mathbf{y}}_{cs,\bar{\tau},\bar{\nu},u,k}$ is then zero mean complex Gaussian with variance:

$$\sigma^2_{1,cs} = 2\sigma^2_A(\frac{\beta C\xi}{M_d})^2|\mathcal{A}_{sc}(\tau_{u,k},\nu_{u,k},\bar{\tau}_{u,k},\bar{\nu}_{u,k})|^2 + 2N_0\frac{C\xi}{M_d}. \tag{11}$$

The proof of (11) follows. Let

$$\sigma^2_{1,cs} = E[\tilde{\mathbf{y}}_{cs,\bar{\tau},\bar{\nu},u,k}\tilde{\mathbf{y}}^*_{cs,\bar{\tau},\bar{\nu},u,k}]$$

taking into account the independence of A_k and $v_{u,k}(m)$ and the independence of $v_{u,k}(m)$ and $v_{u,k}(m')$, $m \neq m'$

$$\sigma^2_{1,cs} = E[A_kA^*_k](\frac{\beta C\xi}{M_d})^2$$

$$\cdot\mathcal{A}_{cs}(\tau_{u,k},\nu_{u,k},\bar{\tau}_{u,k},\bar{\nu}_{u,k})\mathcal{A}^*_{cs}(\tau_{u,k},\nu_{u,k},\bar{\tau}_{u,k},\bar{\nu}_{u,k})$$

$$+\sum_{c=0}^{C-1}\sum_{c'=0}^{C-1}\sum_{m=0}^{M_d-1}E[v_{u,k}(m)v^*_{u,k}(m)]$$

$$\cdot\Phi(c,m)\Phi^*(c',m)s^*_{cs,\bar{\tau},\bar{\nu},u,k}(c)s_{cs,\bar{\tau},\bar{\nu},u,k}(c')$$

which using the fact that $\sum_{m=0}^{M_d-1}\Phi(c,m)\Phi^*(c',m)$ is equal to 1 for $c = c'$ and 0 otherwise (due to the choice of $\mathbf{\Phi}$ to have orthogonal rows as mentioned in Section 2.2), and also using $2\sigma^2_A = E[(A_kA^*_k)]$, $2N_0 = E[v_{u,k}(m)v^*_{u,k}(m)]$ we have

$$\sigma^2_{1,cs} = 2\sigma^2_A(\frac{\beta C\xi}{M_d})^2|\mathcal{A}_{cs}(\tau_{u,k},\nu_{u,k},\bar{\tau}_{u,k},\bar{\nu}_{u,k})|^2$$

$$+2N_0\sum_{c=0}^{C-1}s^*_{cs,\bar{\tau},\bar{\nu},u,k}(c)s_{cs,\bar{\tau},\bar{\nu},u,k}(c)$$

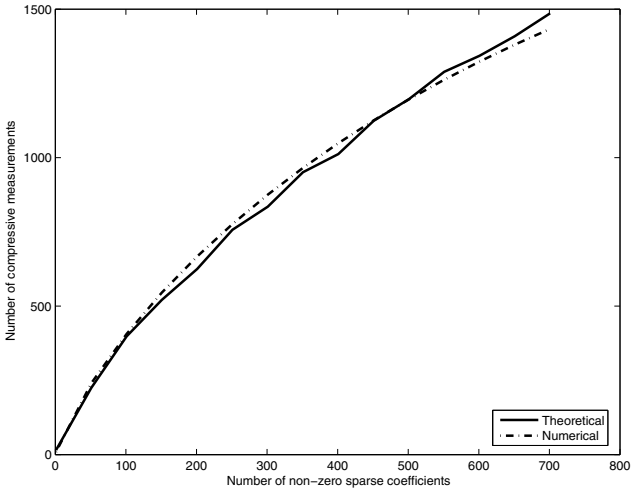

Figure 7: Minimum number of compressive measurements (C) required for reconstruction versus the number of non-zero sparse coefficients ($\mathcal{S}$) to be recovered.

which using (4) the relationship in (11) follows. Similarly when a target is absent $\sigma^2_{0,cs} = 2N_0\frac{\beta C\xi}{M_d}$. The SNR is now $\frac{\beta C}{M_d}\frac{\sigma^2_A\xi}{N_0}$. Therefore, the SNR at the output of the matched filter when using compressive processing is scaled by $\frac{\beta C}{M_d}$ as compared with the SNR when the Nyquist sampled signal is processed. This will in turn have a deteriorating effect on the tracking performance.

Based on the above motion and measurement models the sampling importance resampling (SIR) with the LFM waveform and the likelihood particle filter (LPF) with the CAZAC waveforms [3, 14] are used for radar tracking of a single target. The SIR and LPF particle filtering algorithms are the ones described in detail in [14]. For brevity their description is omitted in this paper.

5 Simulation results

In order to demonstrate recovery of delay-Doppler information from compressive measurements using a nearly orthogonal dictionary the SPGL1 solver [13, 12] was used. The sparsifying dictionary $\mathbf{S}$ (see Section 2.1) used for the reconstruction is a 5199×2121 matrix with columns the delayed and Doppler shifted versions of an $M = 4999$ length Björck CAZAC. The Björck CAZAC was zero padded to length $M_d = 5199$ in order to accommodate a range of delays, while the number of different delay-Doppler shifts allowed was limited to 2121 to reduce memory requirements and the computational expense of the reconstruction process. The range of delays was from 0 to 100 and the Doppler shifts from -10 to 10. The sensing matrix $\mathbf{\Phi}$ (see Section 2.2) is an orthonormal $C \times 5199$ matrix with zero mean and $\frac{1}{M_d}$ variance Gaussian entries created by sampling from a Gaussian distribution followed by orthogonal-triangular decomposition [13]. Figure 7 shows the min-

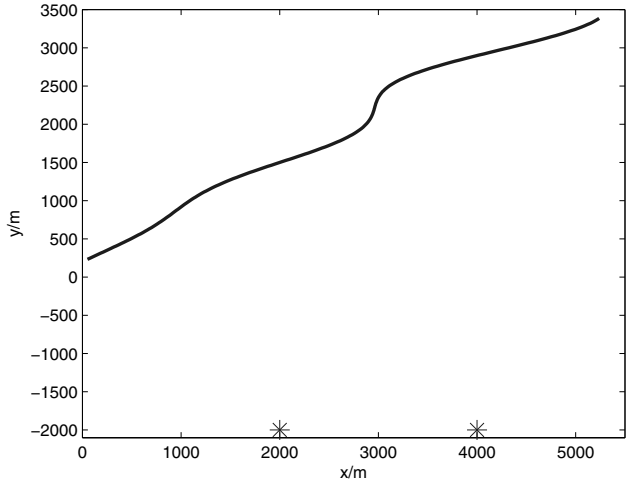

Figure 8: Trajectory of a single target. The two sensors are indicated by a '*'.

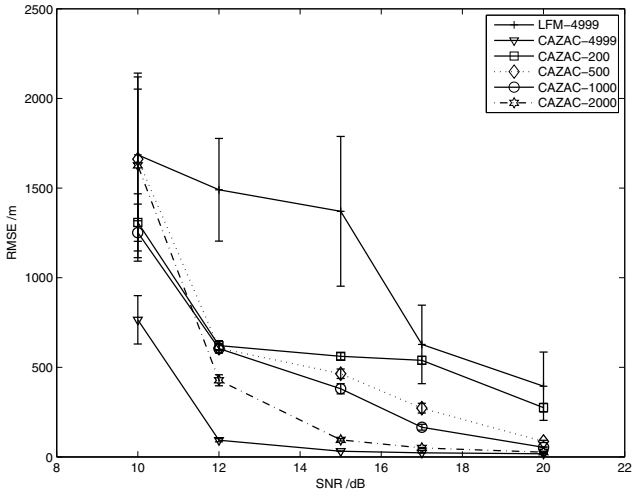

Figure 9: RMSE versus SNR for LFM sequences sampled at Nyquist and CAZAC sequences sampled either at Nyquist or compressively.

imum number of compressive measurements C found to successfully reconstruct the waveform versus the number of non-zero sparse coefficients of the projection of the waveform on the sparsifying dictionary. The maximum allowable reconstruction error for declaring a successful reconstruction, defined as the absolute difference between the reconstructed and original waveform vectors, was set to 10^{-5}. The relationship between the number of compressive measurements and the number of non-zero sparse components agrees with the relationship $C = \alpha \mathcal{S} \log(M_d/\mathcal{S})$ [5] with $\alpha \simeq 2.35$ shown in the plot with a dotted line. Although the purpose of this paper is not to examine reconstruction methods, the ability to reliably reconstruct the CAZAC waveform using a CAZAC dictionary shows that a) the delay-Doppler information is safely embedded in the compressed measurements, and b) that a dictionary based on CAZACs is a reliable sparsifying dictionary that can be used in the reconstruction process.

For the target tracking scenario, a single target moves in a two-dimensional plane in the Cartesian coordinates. The motion is completed in 199 time steps. Two sensors located at $\chi_1 = 2000$ m, $\psi_1 = -2000$ m and $\chi_2 = 4000$ m, $\psi_2 = -2000$ m collect range and range rate measurements. The target is assumed to move according to a nearly constant velocity model with covariance matrix Q =diag(60 7 60 7). The trajectory of the target and the location of the sensors are shown in Figure 8. The SNR varies as $10, 12, 15, 17, 20$ dB. The P_f is set to 10^{-3}, which applies only in the case of the LFM waveform. For the LFM waveform the parameters for starting and ending normalized frequency are $f_a = 0.4$ and $f_b = 0.01$. Both sequences have $M = 4999$ samples, are assumed to be sampled at 10 MHz and frequency modulated by $f_0 = 40$ GHz. In the compressive sensing case, instead of sampling all $M = 4999$ samples of the CAZAC at a high sampling rate only $C = 200, 500, 1000$, or 2000 compressive samples are taken. The velocity of waveform propagation is $v_c = 2.997925 \times 10^8$ m/s.

For the simulations $N = 800$ particles were used and the results were averaged over 100 Monte Carlo runs and the 199 time steps of the scenario. In Figure 9 the RMSE tracking performance is shown for different values of SNR and for both waveforms with a different number of compressive measurements acquired for the CAZAC. One observation is that the use of a Björck CAZAC clearly outperforms tracking with an LFM waveform. It also produces more reliable estimates as shown by the much shorter confidence intervals. In the case of using CAZAC measurements that are obtained compressively, the tracking error performance deteriorates as the number of samples obtained decreases. However, for $C = 200, 500, 1000, 2000$ the performance when using a compressively sensed CAZAC is still better than using the LFM at high data rates. This shows that a compressively sensed and processed CAZAC sequence provides reliable tracking while making high resolution measurements available, greatly simplifying receiver design, and reducing computational expense.

6 Conclusion

In this paper, the feasibility of using compressively sensed and processed waveforms for reliable target tracking was examined. The increase in the AF sidelobes of LFM and CAZAC sequences due to compressive sampling and processing was demonstrated using a numerical based analysis. In addition, theoretical results were derived on the effect of using compressive measurements on the statistical parameters of the matched filter statistic. Moreover, simulation results of

a single target tracking scenario were presented using LFM and CAZAC waveforms sampled at the Nyquist rate and CAZAC waveforms sampled compressively. The results demonstrate the ability to track reliably using compressive measurements of Björck CAZAC sequences with no need for reconstruction. Extensions of this work will examine the combination of adaptive waveform design methods with compressed sensing and processing to further reduce the effect of AF sidelobe degradation and improve tracking performance.

References

[1] N. Levanon and E. Mozeson, "Radar signals," Wiley, 2004.

[2] R. Baraniuk, "Compressive sensing," IEEE Signal Processing Magazine, 24(4), pp. 118-121, July, 2007.

[3] M. S. Arulampalam, S. Maskell, N. Gordon, and T. Clapp "A tutorial on particle filters for online nonlinear/non-Gaussian Bayesian tracking", *IEEE Transactions on Signal Processing*, vol. 50, no. 2, pp. 174-188, Feb. 2002.

[4] E. Candès, J. Romberg, and T. Tao, "Robust uncertainty principles: Exact signal reconstruction from highly incomplete frequency information," IEEE Trans. Inform. Theory, vol. 52, no. 2, pp. 489509, Feb. 2006.

[5] E. Candès and M. Wakin, "An introduction to compressive sampling," IEEE Signal Processing Magazine, 25(2), pp. 21 - 30, March 2008.

[6] D. Donoho, "Compressed sensing," IEEE Trans. Inform. Theory, vol. 52, no. 4, pp. 12891306, Apr. 2006.

[7] R. Baraniuk and P. Steeghs, "Compressive radar imaging," IEEE Radar Conference, pp 128 - 133, April, 2007.

[8] J.A. Tropp, M.B. Wakin, M.F. Duarte, D. Baron, R.G. Baraniuk, "Random filters for compressive sampling and reconstruction," IEEE International Conference on Acoustics, Speech and Signal Processing, vol. 3, May 2006.

[9] M.F. Duarte, M.A. Davenport, M.B. Wakin, R.G. Baraniuk, "Sparse signal detection from incoherent projections," IEEE International Conference on Acoustics, Speech and Signal Processing, vol. 3, May, 2006.

[10] M. Davenport, P. Boufounos, M. Wakin, and R. Baraniuk, "Signal processing with compressive measurements," IEEE J. of Selected Topics in Signal Processing, vol. 4, no. 2, pp. 445 - 460, 2010.

[11] J.A. Tropp and A, Gilbert, "Signal recovery from random measurements via orthogonal matching pursuit," IEEE Trans. on Information Theory, 53(12) pp. 4655-4666, December, 2007.

[12] E. van den Berg and M. P. Friedlander, "Probing the Pareto frontier for basis pursuit solutions," SIAM J. on Scientific Computing, 31(2):890-912, November, 2008.

[13] E. van den Berg and M. P. Friedlander, "SPGL1: A solver for large-scale sparse reconstruction", http://www.cs.ubc.ca/labs/scl/spgl1, June, 2007.

[14] I. Kyriakides, I. Konstantinidis, D. Morrell, J. J. Benedetto, and A. Papandreou-Suppappola, "Target tracking using particle filtering and CAZAC sequences," Waveform Design and Diversity Conference, pp. 367-371, June 2007.

[15] J.J. Benedetto, J. Donatelli, I. Konstantinidis, and C. Shaw, "A Doppler statistic for zero autocorrelation waveforms," *40th Annual Conference on Information Sciences and Systems*, pp. 1403 - 1407, March 2006.

[16] G. Björck, "Functions of modulus one on $\mathbb{Z}_n$ whose Fourier transforms have constant modulus, and cyclic n-roots," *Proc. NATO Adv. Study Inst. on Recent Adv. in Fourier Analysis and its Applications*, J.S. Byrnes and J. L. Byrnes, ed. pp 131-140, 1990.

[17] E. Candès, "Compressive sampling," Int. Congress of Mathematics, 3, pp. 1433-1452, Madrid, Spain, 2006.

[18] R. Baraniuk, M. Davenport, R. DeVore, and M. Wakin, "A simple proof of the restricted isometry property for random matrices", Constructive Approximation, 28(3), pp. 253-263, Dec. 2008.

[19] C. Rago, P. Willett, Y. Bar-Shalom, "Detection-tracking performance with combined waveforms," *IEEE Trans. on Aerospace and Electronic Systems,* vol. 34, no. 2, pp. 612 - 624, April 1998.

[20] E. Cands and T. Tao, Decoding by linear programming, IEEE Trans. Inf. Theory, vol. 51, no. 12, pp. 42034215, Dec. 2005.

[21] M. I. Skolnik, "Introduction to radar systems," McGraw-Hill, 1980.

[22] Ruixin Niu, P. Willett, Y. Bar-Shalom, "Tracking considerations in selection of radar waveform for range and range-rate measurements," *IEEE Trans. on Aerospace and Electronic Systems*, vol. 38, no. 2, pp. 467 - 487, April 2002.